

Weakly Supervised Convolutional Dictionary Learning with Shared and Discriminative Components for Classification

Hao Chen; Yusen Wu; Dayuan Tan

Abstract—Abstract—Convolutional dictionary learning (CDL) has emerged as a powerful tool for signal representation by learning translation-invariant features through convolution operations. While existing CDL methods primarily focus on fully supervised settings, real-world classification tasks often require learning from weakly labeled data where only bag-level annotations are available. In this paper, we propose a novel weakly supervised convolutional dictionary learning framework that jointly learns shared and class-specific components for multi-instance multi-label (MIML) classification. Our model decomposes signals into background patterns captured by a shared dictionary and discriminative features encoded in class-specific dictionaries, with nuclear norm constraints preventing feature dilution. We develop a Block Proximal Gradient method with Majorization (BPG-M) that alternately updates dictionary atoms and sparse coefficients while ensuring convergence to local minima. The proposed method incorporates a projection that aggregates instance-level predictions to bag-level labels through learnable pooling operators. Experimental results on both synthetic and real-world datasets demonstrate that our framework achieves superior classification performance compared to existing MIML methods, particularly in low-label regimes. The learned dictionaries provide interpretable representations while effectively handling background noise and variable-length instances, making the method suitable for applications like environmental sound classification and RF signal analysis.

Index Terms—Dictionary learning, convolutional dictionary learning, weakly supervised learning, multi-instance multi-label learning, classification.

I. INTRODUCTION

Dictionary learning (DL) has emerged as a powerful tool for sparse signal representation, with applications ranging from denoising to data compression [1], [2], [3]. Different from the sparse coding problem with a given dictionary, typically choosing wavelets as the atoms, DL jointly learns sparse coefficients and the atoms from the data. There are two types of dictionary learning: synthesis and analysis dictionary learning [4]. The former learns a data decomposition with dictionary multiplied by sparse coefficients, while the latter learns a projection of the given data to a sparse space. Some DL methods focus on signal classification in supervised learning settings, utilizing labels to manage signal reconstructions

and regularize sparse coefficients to be discriminative using modified Fisher criteria [5], [6].

Recently, Convolutional dictionary learning (CDL), inspired by convolutional neural networks [7], has shown its capability in image reconstruction with advantages such as translation invariance and learning local features without redundancy. CDL methods have been extended along several dimensions: distributed implementations (DiCoDiLe [8]), multi-modal extensions [9], tensor formulations [10], and integration with deep architectures (DeepM2CDL [11]). Some CDL methods target classification [6], [12], [13], [14], but few focus on Multi-Instance Multi-Label (MIML) scenarios, which are common in weakly supervised cases.

In MIML settings, each piece of training data is a bag of instances with a set of labels associated with the bag, meaning the exact labels of individual instances inside the bag are unknown. This is common in domains like Radio Frequency (RF) or audio, where data collected over a period contains multiple signals, but the labels of individual signals are not revealed. For example, in a room with several Wi-Fi and Bluetooth signals, the collected data is a bag of instances with overall labels (Wi-Fi and Bluetooth) known, but the labels of individual instances are unknown.

Our goal is to develop a MIML classification algorithm that can predict the labels of a given bag. Existing CDL methods like DiCoDiLe [8] focus on distributed optimization but assume instance-level labels. Analysis CDL approaches such as [14] handle weak supervision through probabilistic modeling but sacrifice interpretability and direct background modeling. The tensor formulation in [10] shows promise for handling complex data structures but does not address the fundamental challenges of label ambiguity in MIML settings.

We propose a synthesis-based MIML-CDL framework that combines three key innovations:

- Joint learning of shared background and class-specific dictionaries with nuclear norm constraints, extending multi-modal concepts from [9] to weak supervision
- A projection that aggregates instance-level predictions through learnable pooling operators, inspired by deep aggregation in [11] but with explicit dictionary constraints
- Block Proximal Gradient method with Majorization (BPG-M) optimization adapted for weakly supervised CDL, combining the convergence guarantees of [15] with tensor-aware updates similar to [10].

Our experimental validation demonstrates that the proposed method achieves exceptional performance on both synthetic

H. Chen was with the Department of Electrical and Computer Engineering, University of Maryland, Baltimore County.

Y. Wu was with the Department of Computer Science, University of Miami, Miami, FL, 33146 USA (email: yxw1259@miami.edu).

D. Tan was with the Department of Electrical and Computer Engineering, University of Maryland, Baltimore County.

and real-world datasets compared to existing MIML methods, particularly in low-label regimes. The approach maintains interpretability through explicit dictionary learning while handling background noise and variable-length instances - challenges not addressed in distributed [8] or tensor [10] CDL formulations.

The paper is organized as follows: Section IV formalizes the MIML-CDL problem, Section V-A details our BPG-M optimization approach, Section VI discusses tensor extensions, and Section VII presents comprehensive experiments.

II. RELATED WORK

Our work intersects several research domains: dictionary learning, convolutional sparse representations, weakly supervised learning, and multi-instance multi-label classification. This section contextualizes our contributions within these areas.

A. Dictionary Learning and Convolutional Extensions

Dictionary learning has evolved significantly since the seminal K-SVD algorithm [1], which established the foundation for learning overcomplete representations from data. While early approaches focused on reconstruction quality, discriminative dictionary learning methods like FDDL [5], [16], [17] incorporated label information through Fisher discrimination criteria to enhance classification performance. Analysis dictionary learning [4] offered an alternative perspective by learning projections rather than decompositions.

CDL [18], [19] extended these concepts to handle translation invariance in signals, enabling more efficient representation of temporal and spatial patterns. Recent advances in CDL optimization include distributed implementations (DiCoDiLe [8]), which enable scaling to large datasets but lack mechanisms for weak supervision. Our approach builds upon these foundations while introducing novel constraints specifically designed for MIML scenarios.

B. Weakly Supervised Learning in MIML Settings

MIML learning [20] addresses scenarios where training examples consist of bags of instances with only bag-level labels available. Traditional MIML approaches include instance-space transformations [21] and SVM adaptations [22], which require explicit instance separation. More recent deep learning approaches like Deep MIML [23] have shown promise but typically require large labeled datasets and sacrifice interpretability.

Weakly supervised dictionary learning (WSDL) [14] represents an initial attempt to bridge dictionary learning with weak supervision, but focuses on the analysis formulation and lacks mechanisms for handling background components or convolutional structures. Our synthesis-based MIML-CDL framework addresses these limitations through explicit modeling of shared and discriminative components. The separation of shared and discriminative features has proven effective in both traditional and deep learning contexts. Low-rank shared dictionary learning [24] demonstrated that explicitly modeling

common patterns improves classification by reducing feature redundancy. Multi-modal CDL approaches [9] have extended this concept to handle different data types but typically assume strong supervision.

Our approach introduces nuclear norm constraints on the shared dictionary $\mathbf{D}^{(0)}$ to prevent feature dilution—a critical consideration in weakly supervised scenarios where discriminative features might otherwise be absorbed into the background model. This extends concepts from multi-modal learning [9] to the weakly supervised domain, addressing a significant gap in existing literature.

C. Optimization, Aggregation, and Applications

The computational challenges of CDL have inspired various optimization strategies. While ADMM-based approaches [25], [26] provided initial solutions, they often struggle with convergence in non-convex settings. BPG-M [15] offer stronger theoretical guarantees for CDL problems.

Tensor formulations [10] have further enhanced CDL by enabling structured low-rank constraints on activation tensors. Our adaptation of BPG-M for weakly supervised CDL combines the convergence guarantees of [15] with tensor-aware updates inspired by [10], enabling efficient optimization of the challenging objective in (13).

A critical challenge in MIML learning is aggregating instance-level predictions to form bag-level decisions. Deep learning approaches like [23] typically use end-to-end differentiable pooling operations, while traditional methods often rely on simple heuristics like max or average pooling.

Our approach introduces a learnable projection that aggregates instance-level sparse representations through adaptive pooling operators. Unlike deep aggregation in [11], our method maintains explicit dictionary constraints throughout the aggregation process, preserving interpretability while enabling flexible instance-to-bag mappings. This represents a novel middle ground between purely data-driven deep approaches and rigid traditional pooling strategies.

Environmental sound classification presents particular challenges for weakly supervised methods due to temporal variability and background noise. While deep learning approaches [27] have shown success with large labeled datasets, our experiments demonstrate that structured dictionary learning can achieve competitive performance with greater interpretability, particularly in low-data regimes.

Our MIML-CDL framework integrates these research threads through three key innovations: (1) joint learning of shared and class-specific convolutional dictionaries with nuclear norm constraints, (2) learnable projection mechanisms for instance-to-bag prediction aggregation, and (3) BPG-M optimization adapted for weakly supervised settings. This combination addresses fundamental limitations in existing approaches while maintaining computational efficiency and interpretability.

III. BACKGROUND

In this section, we provide the necessary background on dictionary learning, convolutional dictionary learning, and

multi-instance multi-label learning to establish the foundation for our proposed approach.

A. Dictionary Learning

DL is a representation learning technique that aims to find a set of basis vectors (atoms) such that input signals can be represented as sparse linear combinations of these atoms. Formally, given a set of training signals $\mathbf{X} = [\mathbf{x}_1, \mathbf{x}_2, \dots, \mathbf{x}_N] \in \mathbb{R}^{T \times N}$, dictionary learning seeks to find a dictionary $\mathbf{D} \in \mathbb{R}^{T \times K}$ and a sparse coefficient matrix $\mathbf{Z} \in \mathbb{R}^{K \times N}$ such that $\mathbf{X} \approx \mathbf{D}\mathbf{Z}$ and \mathbf{Z} is sparse.

The standard synthesis dictionary learning problem can be formulated as:

$$\min_{\mathbf{D}, \mathbf{Z}} \|\mathbf{X} - \mathbf{D}\mathbf{Z}\|_F^2 + \lambda \|\mathbf{Z}\|_1 \quad \text{subject to} \quad \|\mathbf{d}_k\|_2 \leq 1, \forall k \quad (1)$$

where $\|\cdot\|_F$ denotes the Frobenius norm, $\|\cdot\|_1$ is the ℓ_1 -norm that promotes sparsity, \mathbf{d}_k is the k -th atom in the dictionary, and λ is a regularization parameter that controls the trade-off between reconstruction error and sparsity.

B. Convolutional Dictionary Learning

CDL extends traditional dictionary learning by replacing matrix multiplication with convolution operations. This approach is particularly effective for signals with spatial or temporal structure, as it can capture local patterns that may appear at different locations within the signal.

In CDL, the reconstruction of any given signal \mathbf{x} can be written as:

$$\mathbf{x} \approx \sum_{k=1}^K \mathbf{d}_k * \mathbf{z}_k \quad (2)$$

where $*$ denotes the convolution operation, \mathbf{d}_k represents the k -th atom in the dictionary, and \mathbf{z}_k is the corresponding sparse feature map.

The key advantage of CDL over traditional DL is its translation invariance property, which allows it to detect similar patterns regardless of their position in the signal. This makes CDL particularly suitable for applications in image processing, audio analysis, and other domains where patterns may appear at various locations.

C. Multi-Instance Multi-Label Learning

MIML learning is a weakly supervised learning paradigm where each training example is represented as a bag of instances, and the bag is associated with multiple labels. The relationship between instances and labels is not explicitly provided during training, making MIML a challenging learning scenario.

Formally, in MIML, we have a training set $\{(\mathbf{X}_i, \mathbf{Y}_i)\}_{i=1}^N$, where $\mathbf{X}_i = \{\mathbf{x}_{i1}, \mathbf{x}_{i2}, \dots, \mathbf{x}_{im_i}\}$ is a bag of m_i instances, and $\mathbf{Y}_i \in \{0, 1\}^C$ is a binary vector indicating the presence or absence of C possible labels for the bag \mathbf{X}_i .

The MIML problem is characterized by two key ambiguities:

- Instance-label ambiguity: It is unknown which instances in a bag correspond to which labels.

- Label-correlation ambiguity: The labels may have complex dependencies that need to be modeled.

These ambiguities make MIML particularly challenging but also relevant for many real-world applications where obtaining fine-grained annotations is expensive or impractical. Examples include image classification where an image (bag) contains multiple objects (instances) and is associated with multiple tags (labels), or audio classification where a recording (bag) contains multiple sound events (instances) and is associated with multiple categories (labels).

IV. PROBLEM FORMULATION

A. Dictionary Learning & Convolutional Dictionary Learning

Since the original synthesis DL, as in Eq. III-A, tries to decompose each of the input data \mathbf{X} into a few linear combinations of the learned basis by two matrix multiplications, namely a dictionary by the sparse coefficients, and since synthesis DL targets data reconstruction without any label usage, the plain vanilla DL can be written as:

$$\min_{\mathbf{D}, \mathbf{z}_n} \sum_n \|\mathbf{x}_n - \mathbf{D}\mathbf{z}_n\|_2^2 + \lambda \|\mathbf{z}_n\|_1, \quad \|\mathbf{d}_k\| \leq 1, \quad (3)$$

where \mathbf{D} contains all the possible features of the data saved as atoms and $\lambda \|\cdot\|_1$ is the sparse regularizer. $\|\mathbf{d}_k\| \leq 1$ is introduced here to avoid the scale ambiguity issue. A good signal reconstruction can be easily obtained by the linear combinations of a few certain atoms.

With similar ideas adopted by CDL, instead of matrix multiplication, the convolution operator is applied to the feature learning and signal reconstruction. Let $\mathbf{d}_k \in \mathbb{R}^M$ be the k -th atom in the dictionary $\{\mathbf{d}_k\}_{k=1}^K$ with the total number of K atoms, $\mathbf{s}_{n,k} \in \mathbb{R}^T$ be the corresponding sparse coefficient. The CDL could be formulated as,

$$\min_{\mathbf{D}, \mathbf{s}_n} \sum_n \|\mathbf{x}_n - \mathcal{P}_B \left\{ \sum_{k=1}^K \mathbf{d}_k * \mathbf{s}_{n,k} \right\}\|_2^2 + \lambda \sum_{k=1}^K \|\mathbf{s}_{n,k}\|_1, \quad \|\mathbf{d}_k\| \leq 1, \quad (4)$$

where $*$ denotes the convolution operator, and $\mathcal{P}_B\{\cdot\}$ is a truncation operator pruning the signal of length $M + T - 1$ to T by removing the boundaries. For example, if M is odd, $\mathcal{P}_B\{\tilde{\mathbf{x}}\} := \mathbf{B}\tilde{\mathbf{x}}$, where $\mathbf{B} := \begin{bmatrix} \mathbf{0}_{T \times \frac{M-1}{2}} & \mathbf{I}_{T \times T} & \mathbf{0}_{T \times \frac{M-1}{2}} \end{bmatrix}$. A remarkable change is the atom dimension M does not need to be the same as the dimension of input signal and the sparse coefficients may not necessarily be the same as the atom dimension, which gives a freedom to learn local features. The convolution operator is translation variant so that CDL are capable to learn local features in variety of temporal positions, which means CDL can learn translation invariant features.

B. Discriminative DL & Convolutional Dictionary Learning

As we have seen, the original DL-based data reconstruction is not tailored for classification. For a supervised setting, because the label for each piece of data is available, supposing

the data have a total of C classes, we can partition the data matrix $\mathbf{X} = [\mathbf{X}^{(1)}, \dots, \mathbf{X}^{(C)}]$. In the same way, the dictionary can be formulated as $\mathbf{D} = [\mathbf{D}^{(1)}, \dots, \mathbf{D}^{(C)}] \in \mathbb{R}^{T \times K}$, where $K = K_1 + \dots + K_C$ and sparse coefficients $\mathbf{Z} = [\mathbf{Z}^{(1)}, \dots, \mathbf{Z}^{(C)}] \in \mathbb{R}^{K \times N}$. For a supervised classification problem, FDDL [5] is one of the most popular Discriminative DL methods, which is formulated as:

$$\min_{\mathbf{D}, \mathbf{Z}} r(\mathbf{X}, \mathbf{D}, \mathbf{Z}) + \lambda_1 \|\mathbf{Z}\|_1 + \lambda_2 f(\mathbf{Z}), \quad \|\mathbf{d}_k^{(c)}\| \leq 1 \quad (5)$$

where $r(\mathbf{X}, \mathbf{D}, \mathbf{Z}) = \sum_{c=1}^C \|\mathbf{X}^{(c)} - \mathbf{D}\mathbf{Z}^{(c)}\|_F^2 + \|\mathbf{X}^{(c)} - \mathbf{D}^{(c)}\mathbf{Z}_c^{(c)}\|_F^2 + \sum_{i \neq c} \|\mathbf{D}^{(i)}\mathbf{Z}_i^{(c)}\|_F^2$ is the discriminative fidelity term, which contains the $\mathbf{Z}_c^{(c)}$ and $\mathbf{Z}_i^{(c)}$, namely the corresponding rows of sparse coefficients for label c and labels except c , and the fisher term $f(\mathbf{Z})$ is defined as $f(\mathbf{Z}) = \sum_{c=1}^C \|\mathbf{Z}^{(c)} - \mathbf{M}^{(c)}\|_F - \|\mathbf{M}^{(c)} - \mathbf{M}\|_F + \|\mathbf{Z}\|_F^2$, where $\mathbf{M}^{(c)}$ and \mathbf{M} are composed of the copies of the mean vectors of $\mathbf{Z}^{(c)}$ and \mathbf{Z} respectively.

To solve the classification problem, a CDL framework is proposed in [18]. Unlike the FDDL with discriminative fidelity term and fisher term, [18] specifies that each training sample is postulated to be well reconstructed by the corresponding class atoms. The training formulation is presented as

$$\min_{\{\mathbf{d}_k, \mathbf{s}_{n,k}^{(c)}\}} \sum_n \|\mathbf{x}_n - \sum_{c=1}^C \mathcal{P}_B \left\{ \sum_{k=1}^K \mathbf{d}_k^{(c)} * \mathbf{s}_{n,k}^{(c)} \right\}\|_2^2 + \lambda \sum_{c=1}^C \sum_{k=1}^K \|\mathbf{s}_{n,k}^{(c)}\|_1. \quad s.t. \|\mathbf{d}_k^{(c)}\| \leq 1, \quad (6)$$

As one can see that CDL formulation can be over-complicated with current notation. Let us define a set of notations and operations to simplify the formulation. Let $\mathcal{D} := [\mathcal{D}^{(1)}, \dots, \mathcal{D}^{(C)}] \in \mathbb{R}^{M \times K}$ with each per-class dictionaries $\mathcal{D}^{(c)} \in \mathbb{R}^{M \times K_c}$ for class index $c = 1, 2, \dots, C$, for each sample the sparse coefficients be $\mathbf{S}_n := [\mathbf{S}_n^{(1)}, \dots, \mathbf{S}_n^{(C)}] \in \mathbb{R}^{T \times K}$ with per-class sparse coefficients $\mathbf{S}_n^{(c)} \in \mathbb{R}^{T \times K_c}$, the convolution operator $*$ for the matrices be $\mathbf{H} * \mathbf{Q} := \sum_{l=1}^L \mathcal{P}_B\{\mathbf{h}_l * \mathbf{q}_l\}$, $\mathbf{H} = [\mathbf{h}_1, \dots, \mathbf{h}_L] \in \mathbb{R}^{M \times L}$, $\mathbf{Q} = [\mathbf{q}_1, \dots, \mathbf{q}_L] \in \mathbb{R}^{T \times L}$. So the formulation (6) can be re-written as

$$\min_{\mathbf{D}, \mathbf{S}_n} \sum_n \|\mathbf{x}_n - \mathcal{D} * \mathbf{S}_n\|_2^2 + \lambda \|\mathbf{S}_n\|_1 \quad s.t. \|\mathbf{d}_k^{(c)}\| \leq 1. \quad (7)$$

C. MIML CDL with background handling

Separating the common features from all the learned features will help the discriminative features to achieve better classification performance. To model the background as well as the discriminative components in the mixture, we adopt a similar idea to [24], to learn both the shared dictionary $\mathcal{D}^{(0)} \in \mathbb{R}^{M \times K_0}$ and the discriminative dictionary \mathcal{D} . The overall dictionary is defined as $\bar{\mathcal{D}} := [\mathcal{D}^{(0)}, \mathcal{D}] \in \mathbb{R}^{M \times \bar{K}}$

with $\bar{K} = K_0 + K$. With $\bar{\mathbf{S}}_n := [\mathbf{S}_n^{(0)}, \mathbf{S}_n] \in \mathbb{R}^{T \times \bar{K}}$, the formulation (7) with shared dictionary can be formulated as:

$$\min_{\bar{\mathcal{D}}, \bar{\mathbf{S}}_n} \sum_n \|\mathbf{x}_n - \bar{\mathcal{D}} * \bar{\mathbf{S}}_n\|_2^2 + \lambda \|\bar{\mathbf{S}}_n\|_1 + \mu \|\mathcal{D}^{(0)}\|_*, \quad (8)$$

$$s.t. \|\mathbf{d}_k^{(c)}\| \leq 1, c = 0, \dots, C$$

where $\|\bar{\mathbf{S}}_n\|_1$ is the sum of the absolute values of all entries in $\bar{\mathbf{S}}_n$, which promotes sparsity, and $\|\mathcal{D}^{(0)}\|_*$ is the nuclear norm (sum of singular values) of $\mathcal{D}^{(0)}$, which promotes low rank. Low rankness is necessary to prevent the common dictionary from absorbing discriminant atoms. Otherwise, $\mathcal{D}^{(0)}$ could contain all the discriminative information, which means $\|\mathbf{x}_n - \mathcal{D}^{(0)} * \mathbf{S}_n^{(0)}\|_2^2$ could be very small without the regularizer $\|\mathcal{D}^{(0)}\|_*$.

However, to address the problem with MIML settings, in the sense that $\{\mathbf{x}_n\}_1^N$ cannot be partitioned into C parts, auxiliary label vectors are needed. Specifically, the supervision can be provided in the form of a C -dimensional binary vector $\mathbf{y}_n \in \{0, 1\}^C$, where the c -th element of \mathbf{y}_n is 1 if a class- c signal is present in \mathbf{x}_n , and 0 otherwise. Note that \mathbf{y}_n may be an all-one vector or all-zero vector, which means that \mathbf{x}_n contains all the classes or only background noise.

In the papers [5], [24], they show the importance of using discriminative fidelity, instead of just using per-class reconstruction as in formulation (7). Furthermore, to fit the MIML settings, the discriminative fidelity should have the capability to pick multiple class reconstructions. Now, we introduce our fidelity term $\mathcal{F}(\mathbf{x}_n, \mathbf{y}_n, \bar{\mathcal{D}}, \bar{\mathbf{S}}_n)$ as:

$$\mathcal{F}(\mathbf{x}_n, \mathbf{y}_n, \bar{\mathcal{D}}, \bar{\mathbf{S}}_n) := \|\mathbf{x}_n - \bar{\mathcal{D}} * \bar{\mathbf{S}}_n\|_2^2 + \left\| \mathbf{x}_n - \sum_{c: \mathbf{y}_n^{(c)}=1} \mathcal{D}^{(c)} * \mathbf{S}_n^{(c)} - \mathcal{D}^{(0)} * \mathbf{S}_n^{(0)} \right\|_2^2 + \sum_{c': \mathbf{y}_n^{(c')}=0} \|\mathcal{D}^{(c')} * \mathbf{S}_n^{(c')}\|_2^2, \quad (9)$$

where the first term is the reconstruction error for \mathbf{x}_n using the entire dictionary $\bar{\mathcal{D}}$, the second term is the reconstruction error using the common dictionary for the background and the per-class dictionaries only corresponding to the signal labels that are present in \mathbf{x}_n , and finally the third term is the residual due to the per-class dictionaries for the signal classes that are *not* present in \mathbf{x}_n .

Compared with [5], [24], instead of using the Fisher term for single label classification, we need a label penalty term to match the MIML settings. To predict the class labels \mathbf{y}_n , one possible solution is to project the discriminative sparse signal \mathbf{S}_n to C dimensions and perform ‘‘pooling’’ over time. Specifically, let us define $\mathbf{w}^{(c)} \in \mathbb{R}^{K_c}$, for $c = 1, 2, \dots, C$ and the bias term $\mathbf{b} \in \mathbb{R}^C$. So the projection $\mathbf{W} := \text{bdiag}\{\mathbf{w}^{(1)}, \dots, \mathbf{w}^{(C)}\} \in \mathbb{R}^{K \times C}$ has a block diagonal structure. Then the predicted label $\hat{\mathbf{y}}_n$ is given by:

$$\hat{\mathbf{y}}_n = \frac{1}{1 + e^{\mathcal{P}_P\{\mathbf{S}_n \mathbf{W}\}^\top + \mathbf{b}}} \in \mathbb{R}^C \quad (10)$$

where \cdot^\top denotes transposition and \mathcal{P}_P is a pooling operator, such as the average pooling $\mathcal{P}_{P_{avg}}\{\mathbf{Y}\} = T^{-1} \mathbf{1}_{1 \times T} \mathbf{Y}$ and

$\mathcal{P}_{P_{max}}\{\tilde{\mathbf{Y}}\} = [\max\{\tilde{\mathbf{y}}^{(1)}\}, \dots, \max\{\tilde{\mathbf{y}}^{(C)}\}]^\top$, where $\tilde{\mathbf{y}}^{(c)}$ is the c -th row of $\tilde{\mathbf{Y}}$. The label penalty function $\mathcal{L}(\hat{\mathbf{y}}, \mathbf{y})$ is used to assess the discrepancy between the true label $\mathbf{y} = [y^{(1)}, \dots, y^{(C)}]^\top$ and the predicted label $\hat{\mathbf{y}} = [\hat{y}^{(1)}, \dots, \hat{y}^{(C)}]^\top$ can be chosen, for instance, as the hinge loss:

$$\mathcal{L}_{hg}(\hat{\mathbf{y}}, \mathbf{y}) := \sum_{c=1}^C \max\{0, 1 - 2(\hat{y}^{(c)} - 1)(2y^{(c)} - 1)\} \quad (11)$$

or the cross-entropy loss:

$$\mathcal{L}_{cr}(\hat{\mathbf{y}}, \mathbf{y}) := - \sum_{c=1}^C [y^{(c)} \log \hat{y}^{(c)} + (1 - y^{(c)}) \log(1 - \hat{y}^{(c)})]. \quad (12)$$

Then, the overall optimization problem for training $\bar{\mathcal{D}}, \bar{\mathbf{S}}_n, \mathbf{W}$ and \mathbf{b} , with given N examples $\{\mathbf{x}_n, \mathbf{y}_n\}_{n=1}^N$ can be formulated as:

$$\min_{\bar{\mathcal{D}}, \mathbf{W}, \mathbf{b}} \sum_{n=1}^N \min_{\bar{\mathbf{S}}_n} \left\{ \mathcal{F}(\mathbf{x}_n, \mathbf{y}_n, \bar{\mathcal{D}}, \bar{\mathbf{S}}_n) + \lambda \|\bar{\mathbf{S}}_n\|_1 + \eta \mathcal{L}(\hat{\mathbf{y}}_n, \mathbf{y}_n) \right\} + \mu \|\mathcal{D}^{(0)}\|_*, \quad \text{s.t. } \|\mathbf{d}_k^{(c)}\| \leq 1, c = 0, \dots, C \quad (13)$$

This formulation is based on \mathbf{x}_n being a T -dimensional vector. If each of the input data is a matrix or a high-dimensional tensor, more discussion will be presented in Sec. VI.

V. ALGORITHM DERIVATION

A. BPG-M setup

In this section, we adopt the BPG-M as the method mentioned in [15] to solve the proposed formulation (13). The BPG-M is trying to solve the minimization problem

$$\min F(\mathbf{x}_1, \dots, \mathbf{x}_k) = f(\mathbf{x}_1, \dots, \mathbf{x}_k) + \sum_k^K g_k(\mathbf{x}_k), \quad (14)$$

where f is assumed to be continuously differentiable, but functions g_k with $k = \{1, \dots, K\}$ are not necessarily differentiable. There is no assumption that either f or g_k with $k = \{1, \dots, K\}$ needs to be convex. Suppose ∇f , the gradient of f , is M -Lipschitz continuous, which means ∇f satisfies

$$\|\nabla f(\mathbf{x}) - \nabla f(\mathbf{y})\|_{M^{-1}} \leq \|\mathbf{x} - \mathbf{y}\|_M, \quad \mathbf{x}, \mathbf{y} \in \mathbb{R}^n, \quad \text{where } \|\mathbf{x}\|_M^2 := \mathbf{x}^T \mathbf{M} \mathbf{x}. \quad (15)$$

The f has a quadratic majorization via M -Lipschitz continuous gradients as

$$f(\mathbf{x}) \leq f(\mathbf{y}) + \langle \nabla f(\mathbf{y}), \mathbf{x} - \mathbf{y} \rangle + \frac{1}{2} \|\mathbf{x} - \mathbf{y}\|_M^2 \quad (16)$$

How to choose and calculate the majorization matrix \mathbf{M} will be discussed in the later section V-B. Since there exists an upper bound of f , in order to solve the minimization problem (14), iteratively lowering the upper bound helps to minimize the overall function. The proximal operator with majorization matrix is applied to achieve this goal, with given \mathbf{M} , and the proximal operator is

$$\text{Prox}_g(\mathbf{y}; \mathbf{M}) = \arg \min_{\mathbf{x}} \frac{1}{2} \|\mathbf{x} - \mathbf{y}\|_M^2 + g(\mathbf{x}). \quad (17)$$

Let us define, in the i -th update, for the k -th block, the cost function can be written as

$$f_k^{(i+1)}(\mathbf{x}_k) = f(\mathbf{x}_1^{(i+1)}, \dots, \mathbf{x}_{k-1}^{(i+1)}, \mathbf{x}_k, \mathbf{x}_{k+1}^{(i)}, \dots, \mathbf{x}_K^{(i)}). \quad (18)$$

The update for $\mathbf{x}_k^{(i+1)}$ can be calculated through the following update

$$\begin{aligned} \mathbf{x}_k^{(i+1)} &= \arg \min_{\mathbf{x}_k^{(i)}} \langle \nabla f_k^{(i+1)}(\tilde{\mathbf{x}}_k^{(i)}), \mathbf{x}_k^{(i)} - \tilde{\mathbf{x}}_k^{(i)} \rangle \\ &\quad + \frac{1}{2} \|\mathbf{x}_k^{(i)} - \tilde{\mathbf{x}}_k^{(i)}\|_{\mathbf{M}_k^{(i)}}^2 + g_k(\mathbf{x}_k^{(i)}) \\ &= \text{Prox}_g(\tilde{\mathbf{x}}_k^{(i)} - \mathbf{M}_k^{(i)-1} \nabla f(\tilde{\mathbf{x}}_k^{(i)}); \mathbf{M}_k^{(i)}) \end{aligned} \quad (19)$$

where $\tilde{\mathbf{x}}_k^{(i)} = \mathbf{x}_k^{(i)} + \mathbf{M}_{W_k}^{(i)}(\mathbf{x}_k^{(i)} - \mathbf{x}_k^{(i-1)})$ with the step size $\mathbf{M}_{W_k}^{(i)} = \delta \mathbf{M}_k^{(i)-1/2} \mathbf{M}_k^{(i-1)1/2}$, $0 < \delta < 1$. Then the general BPG-M algorithm can be written in table 1.

There are several benefits of using BPG-M to solve the problem, as claimed in Chun and Fessler's papers [15], [28]. One of them is, unlike FISTA [29], the function g or f does not to be convex. Another attracting attribute is the guarantee of convergence, though it may converge to local minimum. In addition, it claims to be faster than other comparative methods[15], in terms of time complexity and actual calculation time.

Algorithm 1 General BPG-M algorithm

- 1) while i till stop
 - 2) for all k in 1, ..., K
 - 3) Calculate $\mathbf{M}_k^{(i)}$
 - 4) Calculate the step size $\mathbf{M}_{W_k}^{(i)} = \delta \mathbf{M}_k^{(i)-1/2} \mathbf{M}_k^{(i-1)1/2}$, $0 < \delta < 1$
 - 5) Calculate $\tilde{\mathbf{x}}_k^{(i)} = \mathbf{x}_k^{(i)} + \mathbf{M}_{W_k}^{(i)}(\mathbf{x}_k^{(i)} - \mathbf{x}_k^{(i-1)})$
 - 6) Calculate $\mathbf{x}_k^{(i+1)}$

$$= \text{Prox}_g(\tilde{\mathbf{x}}_k^{(i)} - \mathbf{M}_k^{(i)-1} \nabla f(\tilde{\mathbf{x}}_k^{(i)}); \mathbf{M}_k^{(i)})$$

$$= \arg \min_{\mathbf{x}_k^{(i)}} \frac{1}{2} \|\mathbf{x}_k^{(i)} - \nu\|_{\mathbf{M}_k^{(i)}}^2 + g(\mathbf{x}_k^{(i)})$$

where $\nu = \tilde{\mathbf{x}}_k^{(i)} - \mathbf{M}_k^{(i)-1} \nabla f(\tilde{\mathbf{x}}_k^{(i)})$.
 - 7) end for
 - 8) $i = i + 1$
 - 9) end while
-

B. Solving the problem with BPG-M

Firstly, in order to apply BPG-M, convolution calculation needs to be reformulated into matrix multiplication by reforming as a Toeplitz matrix. Then alternately solving each $\mathbf{d}_k^{(0)}, \mathbf{d}_k^{(c)}, \mathbf{s}_{n,k}^{(0)}, \mathbf{s}_{n,k}^{(c)}$ and $\mathbf{w}_k^{(c)}$ by computing the majorizer function and majorizer matrix for each variable. Finally, the algorithm for solving (13) using the BPG-M will be presented. Here we present the method using cross-entropy loss, because it has the capability to show the probability of the label for a given class. The pooling operator is average pooling. For simplicity, the bias term \mathbf{b} update is included in the variable \mathbf{W} , more details can be found in the section V-B4.

1) *Shared dictionary update*: when updating $\mathcal{D}^{(0)}$ with all other variables fixed, the cost function is:

$$\begin{aligned} \min_{\mathbf{d}_k^{(0)}} & \sum_{n=1}^N \|\mathbf{x}_n - \bar{\mathcal{D}} * \bar{\mathbf{S}}_n\|^2 + \mu \|\mathcal{D}^{(0)}\|_* \\ & + \left\| \mathbf{x}_n - \sum_{c: y_{n,c}=1} \mathcal{D}^{(c)} * \mathbf{S}_n^{(c)} - \mathcal{D}^{(0)} * \mathbf{S}_n^{(0)} \right\|^2, \quad (20) \\ \text{s.t.} & \|\mathbf{d}_k^{(0)}\| \leq 1, \end{aligned}$$

which could be rewritten as matrix multiplication using the truncated Toeplitz matrix as $\mathbf{T}_{s_{n,k}^{(0)}} \in \mathbb{R}^{T \times M}$, where $\mathbf{T}_{s_{n,k}^{(0)}}$ can be calculated as

$$\begin{aligned} \mathbf{T}_{s_{n,k}^{(0)}} = \mathcal{P}_B \left\{ \left[\left[\mathbf{0}_{1 \times \frac{M-1}{2}}, \mathbf{s}_{n,k}^{(0)\top} \right]^\top, \right. \right. \\ \left. \left[\mathbf{0}_{1 \times \frac{M-3}{2}}, \mathbf{s}_{n,k}^{(0)\top}, \mathbf{0}_{1 \times 1} \right]^\top, \right. \\ \left. \dots, \left[\mathbf{s}_{n,k}^{(0)\top}, \mathbf{0}_{1 \times \frac{M-1}{2}} \right]^\top \right\}. \quad (21) \end{aligned}$$

The formulation (20) could be rewritten as

$$\begin{aligned} \min_{\mathbf{d}_k^{(0)}} & \sum_{n=1}^N \frac{1}{2} \|2\mathbf{x}_n - \alpha_n - \beta_n - 2\mathbf{T}_{s_{n,k}^{(0)}} \mathbf{d}_k^{(0)}\|_2^2 + \mu \|\mathcal{D}^{(0)}\|_*, \\ \text{s.t.} & \|\mathbf{d}_k^{(0)}\| \leq 1, \quad (22) \end{aligned}$$

where α_n and β_n are respectively defined as $\alpha_n = \mathcal{D} * \mathbf{S}_n + \mathcal{D}^{(0)'} * \mathbf{S}^{(0)'}$ and $\beta_n = \sum_{c=1}^C y_n^{(c)} \mathcal{D}^{(c)} * \mathbf{S}_n^{(c)} + \mathcal{D}^{(0)'} * \mathbf{S}^{(0)'}$. Here $\mathcal{D}^{(0)'}$ and $\mathbf{S}^{(0)'}$ denotes $\mathcal{D}^{(0)'}$ and $\mathbf{S}^{(0)'}$ without $\mathcal{P}_B \left\{ \mathbf{d}_k^{(0)} * \mathbf{s}_{n,k}^{(0)} \right\}$.

Algorithm 1 can be applied to solve this problem (22) with a fixed majorization matrix $\mathbf{M}_{\mathbf{d}_k^{(0)}} = \text{diag} \left\{ \sum_{n=1}^N 4 |\mathbf{T}_{s_{n,k}^{(0)}}|^\top |\mathbf{T}_{s_{n,k}^{(0)}}| \mathbf{1}_{M \times 1} \right\}$ [28], leading to the step size just $\delta \mathbf{I}$. In addition, with $\nu_{\mathbf{d}_k^{(0)}} := \tilde{\mathbf{d}}_k^{(0)} - \mathbf{M}_{\mathbf{d}_k^{(0)}}^{-1} \sum_n 2 \mathbf{T}_{s_{n,k}^{(0)}}^\top (2 \mathbf{T}_{s_{n,k}^{(0)}} \tilde{\mathbf{d}}_k^{(0)} - 2 \mathbf{x}_n + \alpha_n + \beta_n)$ and $\tilde{\mathbf{d}}_k^{(0)}$ calculated by line (5) in Algorithm 1 involving $\mathbf{d}_k^{(0)}$ in previous iteration, the sub-problem for the BPG-M algorithm is to solve the proximal operator, which is

$$\begin{aligned} \mathbf{d}_k^{(0)} = \arg \min_{\mathbf{d}_k^{(0)}} & \frac{1}{2} \|\mathbf{d}_k^{(0)} - \nu_{\mathbf{d}_k^{(0)}}\|_{\mathbf{M}_{\mathbf{d}_k^{(0)}}}^2 + N \mu \|\mathcal{D}^{(0)}\|_*, \\ \text{s.t.} & \|\mathbf{d}_k^{(0)}\| \leq 1. \quad (23) \end{aligned}$$

To solve problem (23), here we applied ADMM [25] and problem (23) can be reformulated as

$$\begin{aligned} \min_{\mathbf{d}_k^{(0)}} & \frac{1}{2} \|\mathbf{d}_k^{(0)} - \nu_{\mathbf{d}_k^{(0)}}\|_{\mathbf{M}_{\mathbf{d}_k^{(0)}}}^2 + N \mu \|\mathbf{O}\|_*, \quad (24) \\ \text{s.t.} & \|\mathbf{d}_k^{(0)}\| \leq 1, \mathcal{D}^{(0)} = \mathbf{O}, \end{aligned}$$

$$\begin{aligned} \min_{\mathbf{d}_k^{(0)}} & \frac{1}{2} \|\mathbf{d}_k^{(0)} - \nu_{\mathbf{d}_k^{(0)}}\|_{\mathbf{M}_{\mathbf{d}_k^{(0)}}}^2 + N \mu \|\mathbf{O}\|_* + \\ & \text{tr}(\mathbf{Y}^\top (\mathbf{O} - \mathcal{D}^{(0)})) + \frac{\rho}{2} \|\mathbf{O} - \mathcal{D}^{(0)}\|_F^2, \quad (25) \\ \text{s.t.} & \|\mathbf{d}_k\| \leq 1. \end{aligned}$$

Now one can solve this problem (25) by the following steps, iteratively until converged: 1. update $\mathbf{d}_k^{(0)}$ by solving the

problem $\min_{\mathbf{d}_k^{(0)}} \frac{1}{2} \|\mathbf{d}_k^{(0)} - \nu_{\mathbf{d}_k^{(0)}}\|_{\mathbf{M}_{\mathbf{d}_k^{(0)}}}^2 + \frac{\rho}{2} \|\mathbf{z}_k - \mathbf{d}_k^{(0)} + \frac{1}{\rho} \mathbf{y}_k\|_2^2$ with the solution for Quadratically Constrained Quadratic Program (QCQP) [30] 2. update \mathbf{O} , through $N \mu \|\mathbf{O}\|_* + \frac{\rho}{2} \|\mathbf{O} - \mathcal{D}^{(0)} + \frac{1}{\rho} \mathbf{Y}\|_F^2$ solved by a singular value thresholding SVT [31] 3. update \mathbf{Y} , simply by $\mathbf{Y} = \mathbf{Y} + \rho(\mathbf{O} - \mathcal{D}^{(0)})$, where $\rho > 1$.

Algorithm 2 Algorithm for shared dictionary update

- 1: Initialize $\bar{\mathcal{D}}, \bar{\mathbf{S}}_n, \mathbf{W}, \mathbf{b}$ with random values
 - 2: **while** not converge **do**
 - 3: /* Update $\mathcal{D}^{(0)}$ */
 - 4: **for all** $\mathbf{d}_k^{(0)}$ in $\mathcal{D}^{(0)}$ **do**
 - 5: Calculate truncated Toeplitz matrix $\mathbf{T}_{s_{n,k}^{(0)}}$ by (21)
 - 6: Calculate majorization matrix $\mathbf{M}_{\mathbf{d}_k^{(0)}} = \text{diag} \left\{ \sum_{n=1}^N 4 |\mathbf{T}_{s_{n,k}^{(0)}}|^\top |\mathbf{T}_{s_{n,k}^{(0)}}| \mathbf{1}_{M \times 1} \right\}$
 - 7: Step size is $\delta \mathbf{I}$
 - 8: **end for**
 - 9: /* Check convergence */
 - 10: **if** overall loss changing rate $\leq \epsilon$ **then**
 - 11: break
 - 12: **end if**
 - 13: **end while**
-

2) *Discriminative dictionary update*: The cost function for each of the $\mathbf{d}_k^{(c)}$ in \mathcal{D} , with all other variables fixed, is the following

$$\begin{aligned} \min_{\mathbf{d}_k^{(c)}} & \sum_{n=1}^N \|\mathbf{x}_n - \bar{\mathcal{D}} * \bar{\mathbf{S}}_n\|^2 + \sum_{c': y_n^{(c')}=0} \|\mathcal{D}^{(c')} * \mathbf{S}_n^{(c')}\|^2 \\ & + \left\| \mathbf{x}_n - \sum_{c: y_n^{(c)}=1} \mathcal{D}^{(c)} * \mathbf{S}_n^{(c)} - \mathcal{D}^{(0)} * \mathbf{S}_n^{(0)} \right\|^2 \\ \text{s.t.} & \|\mathbf{d}_k^{(c)}\| \leq 1, \quad (26) \end{aligned}$$

The formulation (26) is equivalent to

$$\begin{aligned} \min_{\mathbf{d}_k^{(c)}} & \sum_{n=1}^N \|\mathbf{x}_n - \bar{\mathcal{D}} * \bar{\mathbf{S}}_n\|^2 \\ & + \left\| \mathbf{x}_n - \sum_c y_n^{(c)} \mathcal{D}^{(c)} * \mathbf{S}_n^{(c)} - \mathcal{D}^{(0)} * \mathbf{S}_n^{(0)} \right\|^2 \\ & + \sum_c (1 - y_n^{(c)}) \|\mathcal{D}^{(c)} * \mathbf{S}_n^{(c)}\|^2, \quad (27) \\ \text{s.t.} & \|\mathbf{d}_k^{(c)}\| \leq 1, \end{aligned}$$

which could be further reduced to

$$\min_{\mathbf{d}_k^{(c)}} \sum_{n=1}^N \frac{1}{2} \|\mathbf{T}_{s_{n,k}^{(c)}} \mathbf{d}_k^{(c)} - \gamma_n\|_2^2, \quad \text{s.t.} \|\mathbf{d}_k^{(c)}\| \leq 1 \quad (28)$$

where the Toeplitz matrix of $\mathbf{s}_{n,k}^{(c)}$ is defined as

$$\begin{aligned} \mathbf{T}_{s_{n,k}^{(c)}} := \mathcal{P}_B \left\{ \left[\left[\mathbf{0}_{1 \times \frac{M-1}{2}}, \mathbf{s}_{n,k}^{(c)\top} \right]^\top, \right. \right. \\ \left. \left[\mathbf{0}_{1 \times \frac{M-3}{2}}, \mathbf{s}_{n,k}^{(c)\top}, \mathbf{0}_{1 \times 1} \right]^\top, \right. \\ \left. \dots, \left[\mathbf{s}_{n,k}^{(c)\top}, \mathbf{0}_{1 \times \frac{M-1}{2}} \right]^\top \right\}. \quad (29) \end{aligned}$$

and γ_n can be calculated as

$$\begin{aligned} \gamma_n := & \frac{1}{2}(\mathbf{x}_n - \bar{\mathcal{D}}' * \bar{\mathbf{S}}_n' \\ & + y_n^{(c)}(\mathbf{x}_n - \mathcal{D}^{(0)} * \mathbf{S}_n^{(0)} - y_n^{(c)}\mathcal{D}^{(c)'} * \mathbf{S}_n^{(c)'}) \\ & - \sum_{c' \neq c} y_n^{(c')} \mathcal{D}^{(c')} * \mathbf{S}_n^{(c')} \\ & - (1 - y_n^{(c)})((1 - y_n^{(c)})\mathcal{D}^{(c)'} * \mathbf{S}_n^{(c)'}) \\ & + \sum_{c' \neq c} (1 - y_n^{(c')})\mathcal{D}^{(c')} * \mathbf{S}_n^{(c')}), \end{aligned} \quad (30)$$

In the formulation (30), $\bar{\mathcal{D}}' * \bar{\mathbf{S}}_n'$ denotes the $\bar{\mathcal{D}} * \bar{\mathbf{S}}_n$ without the term $\mathcal{P}_B\{\mathbf{d}_k^{(c)} * \mathbf{s}_{n,k}^{(c)}\}$. Similarly, $\mathcal{D}^{(c)'} * \mathbf{S}_n^{(c)'}$ means $\mathcal{D}^{(c)} * \mathbf{S}_n^{(c)}$ without $\mathcal{P}_B\{\mathbf{d}_k^{(c)} * \mathbf{s}_{n,k}^{(c)}\}$. To follow the procedure described in the Algorithm 1, the majorization matrix can be simply $\mathbf{M}_{\mathbf{d}_k^{(c)}} = \text{diag}\{\sum_{n=1}^N |\mathbf{T}_{s_{n,k}^{(c)}}|^\top |\mathbf{T}_{s_{n,k}^{(c)}}| \mathbf{1}_{M \times 1}\}$ and step size just chosen as $\delta \mathbf{I}$. Let us define $\nu_{\mathbf{d}_k^{(c)}} := \tilde{\mathbf{d}}_k^{(c)} - \mathbf{M}_{\mathbf{d}_k^{(c)}}^{-1} \sum_n \mathbf{T}_{s_{n,k}^{(c)}}^\top (\mathbf{T}_{s_{n,k}^{(c)}} \tilde{\mathbf{d}}_k^{(c)} - \gamma_n)$ and $\mathbf{d}_k^{(c)}$ is still calculated by line (5) in Algorithm 1. The last step is to solve the problem

$$\mathbf{d}_k^{(c)} = \arg \min_{\mathbf{d}_k^{(c)}} \frac{1}{2} \|\mathbf{d}_k^{(c)} - \nu_{\mathbf{d}_k^{(c)}}\|_{\mathbf{M}_{\mathbf{d}_k^{(c)}}}^2, \quad \text{s.t. } \|\mathbf{d}_k^{(c)}\| \leq 1. \quad (31)$$

which is still a QCQP problem that can be solved by accelerated Newton's method [15].

3) *Common sparse coefficients update:* In order to update the common sparse coefficients, the cost function for $\mathbf{s}_{n,k}^{(0)}$ can be reformulated as

$$\begin{aligned} \min_{\mathbf{s}_{n,k}^{(0)}} & \|\mathbf{x}_n - \bar{\mathcal{D}} * \bar{\mathbf{S}}_n\|^2 \\ & + \left\| \mathbf{x}_n - \sum_{c: y_n^{(c)}=1} \mathcal{D}^{(c)} * \mathbf{S}_n^{(c)} - \mathcal{D}^{(0)} * \mathbf{S}_n^{(0)} \right\|^2 \\ & + \lambda \|\mathbf{s}_{n,k}^{(0)}\|_1, \end{aligned} \quad (32)$$

$$\min_{\mathbf{s}_{n,k}^{(0)}} \frac{1}{2} \|2\mathbf{x}_n - \alpha_n - \beta_n - 2\mathbf{T}_{\mathbf{d}_k^{(0)}} \mathbf{s}_{n,k}^{(0)}\|_2^2 + \lambda \|\mathbf{s}_{n,k}^{(0)}\|_1. \quad (33)$$

where

$$\begin{aligned} \mathbf{T}_{\mathbf{d}_k^{(0)}} = \mathcal{P}_B \left\{ \left[\left[\mathbf{0}_{1 \times \frac{T-1}{2}}, \mathbf{d}_k^{(0)\top} \right]^\top, \right. \right. \\ \left. \left[\mathbf{0}_{1 \times \frac{T-3}{2}}, \mathbf{d}_k^{(0)\top}, \mathbf{0}_{1 \times 1} \right]^\top, \right. \\ \left. \dots, \left[\mathbf{d}_k^{(0)\top}, \mathbf{0}_{1 \times \frac{T-1}{2}} \right]^\top \right\} \in \mathbb{R}^{T \times T} \end{aligned} \quad (34)$$

is the truncated Toeplitz matrix of $\mathbf{d}_k^{(0)}$. One noticeable feature of updating $\mathbf{s}_{n,k}^{(0)}$ is it could be parallelly computed for each training example index n . Applying BPG-M to solve problem (33), the majorization matrix could be chosen as $\mathbf{M}_{\mathbf{S}^{(0)}} = \text{diag}\{4|\mathbf{T}_{\mathbf{d}_k^{(0)}}|^\top |\mathbf{T}_{\mathbf{d}_k^{(0)}}| \mathbf{1}_{T \times 1}\}$, and the step size is still a constant $\delta \mathbf{I}$. With $\nu_{\mathbf{s}_{n,k}^{(0)}}$ defined as $\nu_{\mathbf{s}_{n,k}^{(0)}} := \tilde{\mathbf{s}}_{n,k}^{(0)} - \mathbf{M}_{\mathbf{S}^{(0)}}^{-1} 2\mathbf{T}_{\mathbf{d}_k^{(0)}}^\top (2\mathbf{T}_{\mathbf{d}_k^{(0)}} \tilde{\mathbf{s}}_{n,k}^{(0)} - 2\mathbf{x}_n + \alpha_n + \beta_n)$ and again $\tilde{\mathbf{s}}_{n,k}^{(0)}$ calculated at line (5) in Algorithm 1. The last step of the BPG-M will solve the following problem

$$\min_{\mathbf{s}_{n,k}^{(0)}} \frac{1}{2} \|\mathbf{s}_{n,k}^{(0)} - \nu_{\mathbf{s}_{n,k}^{(0)}}\|_{\mathbf{M}_{\mathbf{S}^{(0)}}}^2 + \lambda \|\mathbf{s}_{n,k}^{(0)}\|_1. \quad (35)$$

which can be solved by a threshold operator $\Gamma(a, b) := \text{sign}(a) \max(|a| - b, 0)$, where $\max(|a| - b, 0)$ means the maximum value between $|a| - b$ and 0. The solution is simply $\Gamma(\nu_{\mathbf{s}_{n,k}^{(0)}}(i), \lambda \mathbf{M}_{\mathbf{S}^{(0)}}^{-1}(i, i))$, where $\nu_{\mathbf{s}_{n,k}^{(0)}}(i)$ is the i -th element of $\nu_{\mathbf{s}_{n,k}^{(0)}}$ and $\mathbf{M}_{\mathbf{S}^{(0)}}^{-1}(i, i)$ is the element on the i -th row, i -th column of the inversed matrix of $\mathbf{M}_{\mathbf{S}^{(0)}}$.

4) *Projection update:* The loss function is chosen as the cross-entropy loss as mentioned before. With all other variables fixed, the loss function for \mathbf{W} can be written as

$$\begin{aligned} \min_{\mathbf{W}, \mathbf{b}} \sum_{n=1}^N (\mathbf{1} - \mathbf{y}_n)^\top (\mathcal{P}_P\{\mathbf{S}_n \mathbf{W}\} + \mathbf{b}) \\ + \mathbf{1}^\top \log(1 + e^{\mathcal{P}_P\{\mathbf{S}_n \mathbf{W}\} + \mathbf{b}}) \end{aligned} \quad (36)$$

To simplify the optimization, the bias term \mathbf{b} is incorporated into \mathbf{W} . This bias term is crucial for preventing the predicted label probability from being stuck at 0.5 due to zeros in the sparse coefficients. We define $\hat{\mathbf{w}}^{(c)} := [\mathbf{w}^{[c]\top}, b^{(c)}]^\top \in \mathbb{R}^{K+1}$ and $\hat{\mathbf{s}}_n^{(c)} := [\mathcal{P}_P\{\mathbf{s}_n^{(c)}\}, 1]^\top \in \mathbb{R}^{K+1}$. Consequently, the loss function for each $\hat{\mathbf{w}}^{(c)}$ can be expressed as

$$\min_{\hat{\mathbf{w}}^{(c)}} \sum_{n=1}^N -(1 - y_n^{(c)}) (\hat{\mathbf{s}}_n^{(c)\top} \hat{\mathbf{w}}^{(c)}) + \log(1 + e^{\hat{\mathbf{s}}_n^{(c)\top} \hat{\mathbf{w}}^{(c)}}). \quad (37)$$

Using the average pooling operator, the Hessian matrix for $\hat{\mathbf{w}}^{(c)}$ is given by

$$\mathbf{H}_{\hat{\mathbf{w}}^{(c)}} = \sum_{n=1}^N \frac{e^{\hat{\mathbf{s}}_n^{(c)\top} \hat{\mathbf{w}}^{(c)}} \hat{\mathbf{s}}_n^{(c)} \hat{\mathbf{s}}_n^{(c)\top}}{(1 + e^{\hat{\mathbf{s}}_n^{(c)\top} \hat{\mathbf{w}}^{(c)}})^2}. \quad (38)$$

Since $\frac{e^x}{(1+e^x)^2} \leq \frac{1}{4}$, the majorization matrix for $\hat{\mathbf{w}}^{(c)}$ can be chosen as $\mathbf{M}_{\hat{\mathbf{w}}^{(c)}} = \frac{1}{4} \text{diag}\{\sum_{n=1}^N |\hat{\mathbf{s}}_n^{(c)}| |\hat{\mathbf{s}}_n^{(c)\top}| \mathbf{1}_{(K+1) \times 1}\}$ with step size $\delta \mathbf{I}$. $\nu_{\hat{\mathbf{w}}^{(c)}}$ is then defined as

$$\nu_{\hat{\mathbf{w}}^{(c)}} = \tilde{\mathbf{w}}^{(c)} + \mathbf{M}_{\hat{\mathbf{w}}^{(c)}}^{-1} \sum_{n=1}^N \left[(1 - y_n^{(c)}) \hat{\mathbf{s}}_n^{(c)} - \frac{e^{\hat{\mathbf{s}}_n^{(c)\top} \tilde{\mathbf{w}}^{(c)}}}{1 + e^{\hat{\mathbf{s}}_n^{(c)\top} \tilde{\mathbf{w}}^{(c)}}} \hat{\mathbf{s}}_n^{(c)} \right] \quad (39)$$

where $\tilde{\mathbf{w}}^{(c)}$ is obtained from line (5) in Algorithm 1, based on the previous $\hat{\mathbf{w}}^{(c)}$. The last step of BPG-M directly updates $\hat{\mathbf{w}}^{(c)}$ as $\nu_{\hat{\mathbf{w}}^{(c)}}$.

5) *Distinctive sparse coefficients update:* Similar to the common sparse coefficients update, the update for each $\mathbf{s}_{n,k}^{(c)}$ can be done in a parallel manner. Let's define $\mathbf{p} := T^{-1} \mathbf{1}_{T \times 1}$ and $\hat{\mathbf{s}}_n^{(c)}$ can be written as $\hat{\mathbf{s}}_n^{(c)} = [\mathbf{p}^\top \mathbf{s}_n^{(c)}, 1]^\top$. Let the truncated Toeplitz matrix of $\mathbf{d}_k^{(c)}$ be defined as

$$\begin{aligned} \mathbf{T}_{\mathbf{d}_k^{(c)}} = \mathcal{P}_B \left\{ \left[\left[\mathbf{0}_{1 \times \frac{T-1}{2}}, \mathbf{d}_k^{(c)\top} \right]^\top, \right. \right. \\ \left. \left[\mathbf{0}_{1 \times \frac{T-3}{2}}, \mathbf{d}_k^{(c)\top}, \mathbf{0}_{1 \times 1} \right]^\top, \right. \\ \left. \dots, \left[\mathbf{d}_k^{(c)\top}, \mathbf{0}_{1 \times \frac{T-1}{2}} \right]^\top \right\} \in \mathbb{R}^{T \times T} \end{aligned} \quad (40)$$

To update $\mathbf{s}_{n,k}^{(c)}$, we solve the following minimization problem:

$$\begin{aligned} \min_{\mathbf{s}_{n,k}^{(c)}} \frac{1}{2} \|\mathbf{T}_{\mathbf{d}_k^{(c)}} \mathbf{s}_{n,k}^{(c)} - \gamma_n\|_2^2 + \lambda \|\mathbf{s}_{n,k}^{(c)}\|_1 \\ + \eta (1 - y_n^{(c)}) (\mathbf{p}^\top \mathbf{s}_{n,k}^{(c)} w_k^{(c)}) \\ + \eta \log(1 + e^{\hat{\mathbf{s}}_n^{(c)\top} \hat{\mathbf{w}}^{(c)}}). \end{aligned} \quad (41)$$

The Hessian matrix for $\mathbf{s}_{n,k}^{(c)}$ is given by

$$\mathbf{H}_{\mathbf{s}_{n,k}^{(c)}} = 2\mathbf{T}_{d_k^{(c)}}^\top \mathbf{T}_{d_k^{(c)}} + \eta \frac{e^{\hat{\mathbf{s}}_n^{(c)\top} \hat{\mathbf{w}}^{(c)}}}{(1 + e^{\hat{\mathbf{s}}_n^{(c)\top} \hat{\mathbf{w}}^{(c)}})^2} (w_k^{(c)})^2 \mathbf{p}\mathbf{p}^\top, \quad (42)$$

where $w_k^{(c)}$ is the k -th element of vector $\mathbf{w}^{(c)}$ and is a scalar. The majorization matrix is chosen as $\mathbf{M}_{\mathbf{S}^{(c)}} = \text{diag}(4\mathbf{T}_{d_k^{(c)}}^\top \mathbf{T}_{d_k^{(c)}} + \eta \frac{1}{4} (w_k^{(c)})^2 \mathbf{p}\mathbf{p}^\top)$. In the last step of the BPG-M algorithm, we solve the problem (43) using the threshold operator Γ .

$$\min_{\mathbf{s}_{n,k}^{(c)}} \frac{1}{2} \|\mathbf{s}_{n,k}^{(c)} - \nu_{\mathbf{s}_{n,k}^{(c)}}\|_{\mathbf{M}_{\mathbf{S}^{(c)}}}^2 + \lambda \|\mathbf{s}_{n,k}^{(c)}\|_1. \quad (43)$$

where $\nu_{\mathbf{s}_{n,k}^{(c)}}$ is calculated as follows:

$$\begin{aligned} \nu_{\mathbf{s}_{n,k}^{(c)}} &= \tilde{\mathbf{s}}_{n,k}^{(c)} - \mathbf{M}_{\mathbf{S}^{(c)}}^{-1} (2\mathbf{T}_{d_k^{(c)}}^{(c)\top} (\mathbf{T}_{d_k^{(c)}} \tilde{\mathbf{s}}_{n,k}^{(c)} - \gamma_n) \\ &\quad + \eta(1 - y_n^{(c)}) w_k^{(c)} \mathbf{p} \\ &\quad + \eta(1 + e^{\hat{\mathbf{s}}_n^{(c)\top} \hat{\mathbf{w}}^{(c)}})^{-1} \\ &\quad \times e^{\hat{\mathbf{s}}_n^{(c)\top} \hat{\mathbf{w}}^{(c)}} w_k^{(c)} \mathbf{p} \end{aligned} \quad (44)$$

where $\hat{\mathbf{s}}_n^{(c)} = [\mathbf{p}^\top \tilde{\mathbf{s}}_n^{(c)}, 1]^\top$ and $\tilde{\mathbf{s}}_{n,k}^{(c)}$ is obtained from the previous steps during the BPG-M calculation. The overall algorithm to solve problem (13) is listed in table I.

VI. EXTENSION TO TENSOR DATA

In previous sections, we represented the n -th bag of data as $\mathbf{x}_n \in \mathbb{R}^T$, where each instance is a 1-D vector and the bag of instances is concatenated sequentially. For the proposed MIML-CDL model (13), the k -th atom in the c -th class is $\mathbf{d}_k^{(c)} \in \mathbb{R}^M$ with its corresponding sparse coefficient $\mathbf{s}_{n,k}^{(c)} \in \mathbb{R}^T$ for the n -th bag in the c -th class. While high-dimensional data can be vectorized into 1-D representations, such vectorization causes significant loss of structural information during convolution operations. For instance, a 2-D image processed with a 2-D convolution kernel naturally captures both vertical and horizontal patterns. However, when the same image is vectorized horizontally, a 1-D convolution can only extract horizontal patterns, completely missing vertical relationships. This structural information loss due to vectorization leads to degraded classification performance. Therefore, extending our proposed model to handle high-dimensional data in its native format is essential for preserving spatial relationships and achieving optimal classification results.

A. Tensor data

The proposed model naturally extends to higher-dimensional data through tensor formulations. Consider first a 2D bag representation $\mathbf{X}_n \in \mathbb{R}^{F \times T}$, where instances are temporally concatenated along the second dimension (alternative instance configurations will be discussed in Section VI-B). Let the j -th instance in the n -th bag be $\mathbf{I}_{n,j} \in \mathbb{R}^{F \times T_j}$ with $\sum_j T_j = T$. Each dictionary atom for class c becomes a 2D filter $\mathcal{D}_k^{(c)} \in \mathbb{R}^{F \times M}$, while the corresponding sparse coefficients $\mathbf{s}_{n,k}^{(c)} \in \mathbb{R}^T$ retain their original dimensionality.

This formulation generalizes to arbitrary dimensions through tensor notation. For an N -dimensional tensor bag $\overrightarrow{\mathbf{X}}_n \in \mathbb{R}^{T_1 \times \dots \times T_N}$, the c -th class dictionary atoms become N -dimensional tensors $\mathcal{D}_k^{(c)} \in \mathbb{R}^{T_1 \times \dots \times T_{N-1} \times M}$, while the sparse coefficients $\mathbf{s}_{n,k}^{(c)} \in \mathbb{R}^T$ maintain their original vector form. Crucially, the coefficient dimensionality remains invariant to the input dimension, preserving the pooling operation's compatibility.

For implementations, we note that current majorization matrix computations support up to 2D operations. Higher-dimensional data (3D+) can be handled by preserving two principal dimensions and collapsing remaining dimensions through reindexing. Formally, this amounts to reshaping a tensor $\overrightarrow{\mathbf{X}} \in \mathbb{R}^{T_1 \times \dots \times T_D}$ into a matrix $\mathbf{X}' \in \mathbb{R}^{T_1 \times (\prod_{d=2}^D T_d)}$, effectively decomposing the high-dimensional structure into separate 2D slices while preserving the model's core functionality.

B. Separated instances in a bag

When handling separated instances in a bag, two distinct scenarios arise: 1) Instances may be small patches extracted from a larger bag data (e.g., a single image containing both cats and dogs, where individual animal regions constitute separate instances), or 2) Instances may be independent data elements (e.g., a collection of separate images, each representing one instance in the bag).

For the first scenario, our model must adaptively adjust the dimensions of atoms and sparse coefficients. Given a 2-dimensional bag $\mathbf{X}_n \in \mathbb{R}^{F \times T}$, the j -th instance in the n -th bag becomes $\mathbf{I}_{n,j} \in \mathbb{R}^{F_j \times T_j}$, where $\sum_j F_j \leq F$ and $\sum_j T_j \leq T$. Consequently, each atom in the c -th class is defined as $\mathcal{D}_k^{(c)} \in \mathbb{R}^{\max(\{F_j\}_j) \times \max(\{T_j\}_j)}$, with corresponding sparse coefficients $\mathbf{s}_{n,k}^{(c)} \in \mathbb{R}^{F \times T}$. The model structure remains unchanged except for adjustments to the dimensionality of the pooling operator and majorization matrix.

In the second scenario, where instances are independent data elements, the n -th sample is represented as $\mathbf{X}_n = \{\mathbf{I}_{n,j}\}_{j=1}^J$, with each instance $\mathbf{I}_{n,j} \in \mathbb{R}^{F \times T}$. The atoms for the c -th class maintain their form as $\mathcal{D}_k^{(c)} \in \mathbb{R}^{F \times M}$, while the sparse coefficients are denoted as $\mathbf{s}_{n,k,j}^{(c)} \in \mathbb{R}^T$ for the n -th bag, c -th class, k -th atom, and j -th instance. The computational pipeline remains consistent with our original formulation, with the key modification being that the pooling operation now operates on the concatenation of all J instance coefficients $\mathbf{s}_{n,k,j}^{(c)}$.

VII. NUMERICAL EXPERIMENTS

In this section, we evaluate our proposed algorithm on both synthetic and real-world datasets to demonstrate its effectiveness. We implemented our approach with support for both CPU and GPU acceleration, and the complete source code is available on GitHub¹. We present comprehensive results including classification performance metrics, detailed numerical analysis, and comparisons against state-of-the-art related works.

¹<https://github.com/chenhao1umbc/WSCDL>

TABLE I
MIML-CDL TRAINING ALGORITHM DETAILS

Initialize $\mathcal{D}, \mathbf{S}_n, \mathbf{W}, \mathbf{b}$ with random values

while not converge:
 /* Update $\mathcal{D}^{(0)}$ */
for all $\mathbf{d}_k^{(0)}$ in $\mathcal{D}^{(0)}$:
 Calculate truncated Toeplitz matrix $\mathbf{T}_{s_{n,k}^{(0)}}$ by (21)
 Calculate majorization matrix $\mathbf{M}_{\mathbf{d}_k^{(0)}} = \text{diag}\{\sum_{n=1}^N 4|\mathbf{T}_{s_{n,k}^{(0)}}|^\top |\mathbf{T}_{s_{n,k}^{(0)}}| \mathbf{1}_{M \times 1}\}$, step size is $\delta \mathbf{I}$
 Using Algorithm 1 to solve $\min_{\mathbf{d}_k^{(0)}} \sum_{n=1}^N \frac{1}{2} \|2\mathbf{x}_n - \alpha_n - \beta_n - 2\mathbf{T}_{s_{n,k}^{(0)}} \mathbf{d}_k^{(0)}\|_2^2 + \mu \|\mathcal{D}^{(0)}\|_*, \text{ s.t. } \|\mathbf{d}_k^{(0)}\| \leq 1$
 The last step of Algorithm 1 is to solve $\min_{\mathbf{d}_k^{(0)}} \frac{1}{2} \|\mathbf{d}_k^{(0)} - \nu_{\mathbf{d}_k^{(0)}}\|_{\mathbf{M}_{\mathbf{d}_k^{(0)}}}^2 + N\mu \|\mathcal{D}^{(0)}\|_*, \text{ s.t. } \|\mathbf{d}_k^{(0)}\| \leq 1$.
 /* solve the last step by ADMM equivalent to solve (25) */
while not converge:
 1. update $\mathbf{d}_k^{(0)}$ through $\min_{\mathbf{d}_k^{(0)}} \frac{1}{2} \|\mathbf{d}_k^{(0)} - \nu_{\mathbf{d}_k^{(0)}}\|_{\mathbf{M}_{\mathbf{d}_k^{(0)}}}^2 + \frac{\rho}{2} \|\mathbf{z}_k - \mathbf{d}_k^{(0)} + \frac{1}{\rho} \mathbf{y}_k\|_2^2$ using QCQP
 2. update \mathbf{O} through $N\mu \|\mathbf{O}\|_* + \frac{\rho}{2} \|\mathbf{O} - \mathcal{D}^{(0)} + \frac{1}{\rho} \mathbf{Y}\|_F^2$ using SVT
 3. update \mathbf{Y} , simply by $\mathbf{Y} = \mathbf{Y} + \rho(\mathbf{O} - \mathcal{D}^{(0)})$, where $\rho > 1$.
 4. Check convergence $\|\mathbf{O} - \mathcal{D}^{(0)}\| \leq \epsilon$

/* Update \mathcal{D} */
for all $\mathbf{d}_k^{(c)}$ in \mathcal{D} :
 Calculate truncated Toeplitz matrix $\mathbf{T}_{s_{n,k}^{(c)}}$ by (29)
 Calculate majorization matrix $\mathbf{M}_{\mathbf{d}_k^{(c)}} = \text{diag}\{\sum_{n=1}^N |\mathbf{T}_{s_{n,k}^{(c)}}|^\top |\mathbf{T}_{s_{n,k}^{(c)}}| \mathbf{1}_{M \times 1}\}$, step size is $\delta \mathbf{I}$
 Using Algorithm 1 to solve $\min_{\mathbf{d}_k^{(c)}} \sum_{n=1}^N \frac{1}{2} \|\mathbf{T}_{s_{n,k}^{(c)}} \mathbf{d}_k^{(c)} - \gamma_n\|_2^2, \text{ s.t. } \|\mathbf{d}_k^{(c)}\| \leq 1$
 The last step of Algorithm 1 is to solve $\min_{\mathbf{d}_k^{(c)}} \frac{1}{2} \|\mathbf{d}_k^{(c)} - \nu_{\mathbf{d}_k^{(c)}}\|_{\mathbf{M}_{\mathbf{d}_k^{(c)}}}^2, \text{ s.t. } \|\mathbf{d}_k^{(c)}\| \leq 1$ by accelerated Newton's method.

/* Update $\mathbf{S}_n^{(0)}$ */
for all $\mathbf{s}_{n,k}^{(0)}$ in $\mathbf{S}_n^{(0)}$:
 Calculate truncated Toeplitz matrix $\mathbf{T}_{d_k^{(0)}}$ by (34)
 Calculate majorization matrix $\mathbf{M}_{\mathbf{S}^{(0)}} = \text{diag}\{4|\mathbf{T}_{d_k^{(0)}}|^\top |\mathbf{T}_{d_k^{(0)}}| \mathbf{1}_{T \times 1}\}$, step size is $\delta \mathbf{I}$
 Using Algorithm 1 to solve $\min_{\mathbf{s}_{n,k}^{(0)}} \frac{1}{2} \|2\mathbf{x}_n - \alpha_n - \beta_n - 2\mathbf{T}_{d_k^{(0)}} \mathbf{s}_{n,k}^{(0)}\|_2^2 + \lambda \|\mathbf{s}_{n,k}^{(0)}\|_1$
 The last step of Algorithm 1 is to solve $\min_{\mathbf{s}_{n,k}^{(0)}} \frac{1}{2} \|\mathbf{s}_{n,k}^{(0)} - \nu_{\mathbf{s}_{n,k}^{(0)}}\|_{\mathbf{M}_{\mathbf{S}^{(0)}}}^2 + \lambda \|\mathbf{s}_{n,k}^{(0)}\|_1$, by thresholding operator.

/* Update \mathbf{S}_n */
for all $\mathbf{s}_{n,k}^{(c)}$ in $\mathbf{S}_n^{(c)}$:
 Calculate truncated Toeplitz matrix $\mathbf{T}_{d_k^{(c)}}$ by (40)
 Calculate majorization matrix $\mathbf{M}_{\mathbf{S}^{(c)}} = \text{diag}\{|\mathbf{M}_{\mathbf{S}}|^\top |\mathbf{M}_{\mathbf{S}}| \mathbf{1}_{T \times 1}\}$, where $\mathbf{M}_{\mathbf{S}} = [2\mathbf{T}_{d_k^{(c)}}^\top, \frac{1}{2}\sqrt{\eta}\mathbf{p}|w_k^{(c)}|]^\top$, step size is $\delta \mathbf{I}$
 Using Algorithm 1 to solve $\min_{\mathbf{s}_{n,k}^{(c)}} 2\|\mathbf{T}_{d_k^{(c)}} \mathbf{s}_{n,k}^{(c)} - \gamma_n\|_2^2 + \lambda \|\mathbf{s}_{n,k}^{(c)}\|_1 + \eta(1 - y_n^{(c)})(\mathbf{p}^\top \mathbf{s}_{n,k}^{(c)} w_k^{(c)} + \eta \log(1 + e^{(\hat{\mathbf{s}}_n^{(c)\top} \hat{\mathbf{w}}^{(c)})})$.
 The last step of Algorithm 1 is to solve $\min_{\mathbf{s}_{n,k}^{(c)}} \frac{1}{2} \|\mathbf{s}_{n,k}^{(c)} - \nu_{\mathbf{s}_{n,k}^{(c)}}\|_{\mathbf{M}_{\mathbf{S}^{(c)}}}^2 + \lambda \|\mathbf{s}_{n,k}^{(c)}\|_1$, by thresholding operator.

/* Update \mathbf{W} and \mathbf{b} */
for all $\mathbf{w}^{(c)}$ in \mathbf{W} :
 Calculate majorization matrix $\mathbf{M}_{\hat{\mathbf{w}}^{(c)}} = \frac{1}{4} \text{diag}\{\sum_{n=1}^N |\hat{\mathbf{s}}_n^{(c)}| |\hat{\mathbf{s}}_n^{(c)\top}| \mathbf{1}_{(K+1) \times 1}\}$, step size is $\delta \mathbf{I}$
 Using Algorithm 1 to solve $\min_{\hat{\mathbf{w}}^{(c)}} \sum_{n=1}^N -(1 - y_n^{(c)}) (\hat{\mathbf{s}}_n^{(c)\top} \hat{\mathbf{w}}^{(c)}) + \log(1 + e^{\hat{\mathbf{s}}_n^{(c)\top} \hat{\mathbf{w}}^{(c)}})$.

/* Check convergence */
if the overall loss changing rate $\leq \epsilon$, break

A. Synthetic data

We created a synthetic 1D dataset with 4 classes plus background signals. Each class and background has 5 base features (30 samples each) using sinusoids and saw-tooth waveforms. Features appear as bursts (up to 5 consecutive repetitions) separated by variable-length zero-padded intervals. Each example is a 1600-sample time series containing random bursts.

We generated all 15 possible multi-label combinations from the 4 classes. The test set contains 50 examples per combination (750 total), while the training set (550 examples) deliberately excludes single-label examples to challenge the algorithm to learn without single-label supervision. We added white Gaussian noise (10 dB SNR) to test robustness. Labels are represented as binary vectors indicating class presence.

Fig. 1(c) visualizes the first 50 samples of the first 50 training examples, with time indices along the x-axis and

example indices along the y-axis.

For our implementation, we employ average pooling as the pooling operator and cross-entropy loss as the objective function. The BPG-M optimization algorithm guarantees convergence to a local minimum with rapid convergence properties. As shown in Fig. 2, the loss function decreases significantly during the first 10 epochs, reaching approximately one-third of its initial value. The loss continues to decrease monotonically throughout training, eventually stabilizing at a local minimum around epoch 40. This efficient convergence behavior demonstrates the effectiveness of our optimization approach. The quality of the learned dictionary atoms is evident in the reconstruction results, which successfully remove noise and closely match the ground-truth data, as illustrated in Fig. 1(a) and Fig. 1(b).

Fig. 3 compares the learned dictionary atoms (blue line) with ground-truth features (orange with "x" markers). Despite

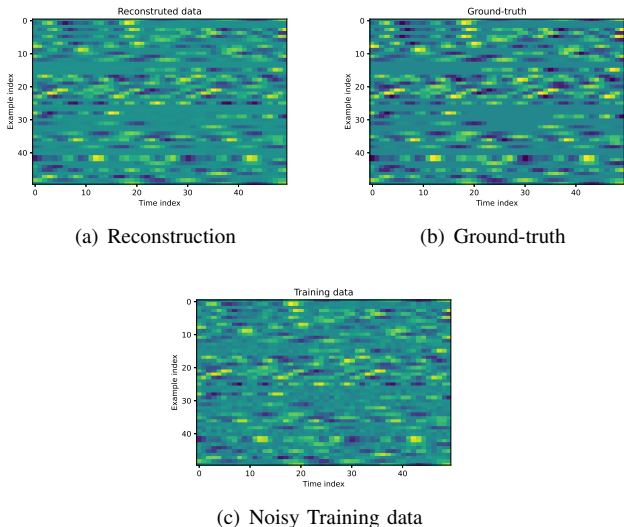


Fig. 1. Comparison of reconstructed data and training data. (a) The reconstructed data is clean with Gaussian noise removed. (b) The ground truth data without noise. (c) The first 50 samples of the first 50 training data

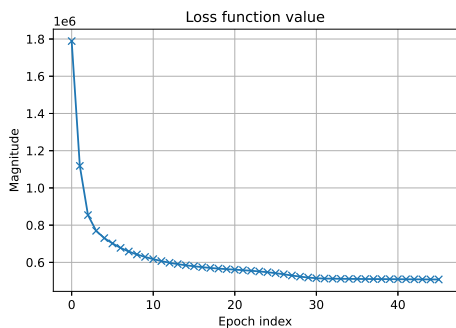


Fig. 2. Loss function value versus training epochs. The loss decreases rapidly in the first 10 epochs and continues to decrease more gradually until reaching a local minimum around epoch 40, showing the fast convergence of the proposed algorithm.

the absence of single-label examples in training, all features—including class-specific and background features—are correctly identified through the label penalty and sparsity constraints. Some learned features exhibit circular shifts (e.g., feature 1 shows a 15-sample shift and feature 4 a 2-sample shift) due to truncation in the generated data. Importantly, these shifts don’t compromise reconstruction quality because of the translation invariance property of convolution.

Fig. 4 presents the testing results, where each sub-figure shows class indices (x-axis) against test example indices (y-axis). Despite not being trained on single-label examples, our model successfully identifies them during testing. Using a threshold of 0.5 for classification decisions (Fig. 4(c)), the model achieves an impressive accuracy of 0.9827.

B. Public real-world data

We evaluate our method on ESC-10, a curated subset of the ESC-50 dataset [32] containing 10 environmental sound classes (Chainsaw, Clock tick, Cracking fire, Crying baby,

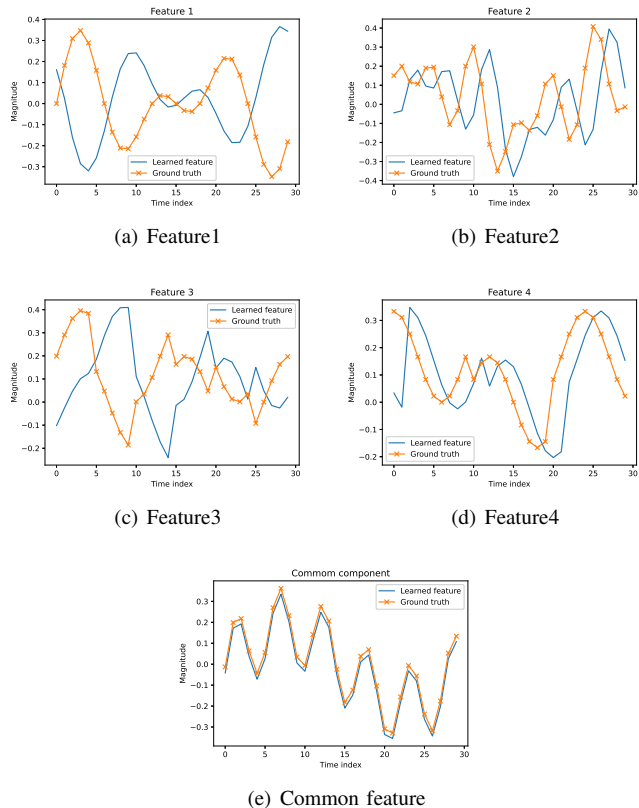


Fig. 3. The per-class feature and common feature are shown in (a)-(e) respectively. The learned features are labeled correctly with some time shifts, due to the burst feature and truncated data.

Dog, Helicopter, Rain, Rooster, Sea waves, and Sneezing). Each recording is a 5-second audio clip sampled at 44.1kHz. To create a weakly supervised setting, we organized 5,000 instances into 1,000 bags with 5 instances per bag, where each instance could be either a sound from ESC-10 or null. We transformed the audio data into 100×100 time-frequency representations using Short-Time Fourier Transform (STFT) and downsampling. Fig. 5 shows an example bag with five concatenated instances (indices 0-99, 100-199, 200-299, 300-399, and 400-499) labeled as ”Sneezing,” ”Sea waves,” ”Cracking fire,” ”Sneezing,” and ”Null” respectively. The y-axis represents frequency (with lower frequencies at the top), and we display only the one-sided spectrum due to the symmetry of the STFT.

The comparison of performance is conducted among several weakly supervised methods: WSDL [14], our proposed WCDL, MIML-SVM [20], [22], MIML-kNN [21], and Deep MIML network [23]. We divided the dataset into 800 bags for training/validation and 200 bags for testing. For validation, we employed 5-fold cross-validation with 160 bags per fold. For MIML-SVM and MIML-kNN, which require separated instances in each bag, we followed the scenario 2 described in Section VI-B, while Deep MIML network corresponds to scenario 1.

For this multi-label classification task, we evaluated performance using accuracy, recall, precision, F1-score, and Area Under Curve (AUC). After hyperparameter tuning, MIML-

	Accuracy	Recall	Precision	F1 score	AUC
Deep MIML	0.5432	0.2918	0.4029	0.3321	0.5119
MIML-kNN	0.5307	0.6035	0.3927	0.4719	0.5230
MIML-SVM (linear)	0.6247	0.5579	0.5062	0.5307	0.6639
MIML-SVM (RBF)	0.6207	0.4950	0.5037	0.4991	0.6628
WSDL	0.5405	0.2956	0.3837	0.3878	0.5050
WSCDL(ours)	0.6330	0.5506	0.5321	0.5423	0.6753

TABLE II
COMPARISON OF CLASSIFICATION PERFORMANCE METRICS ACROSS DIFFERENT WEAKLY SUPERVISED METHODS ON THE ESC-10 DATASET. BEST RESULTS ARE HIGHLIGHTED IN BOLD.

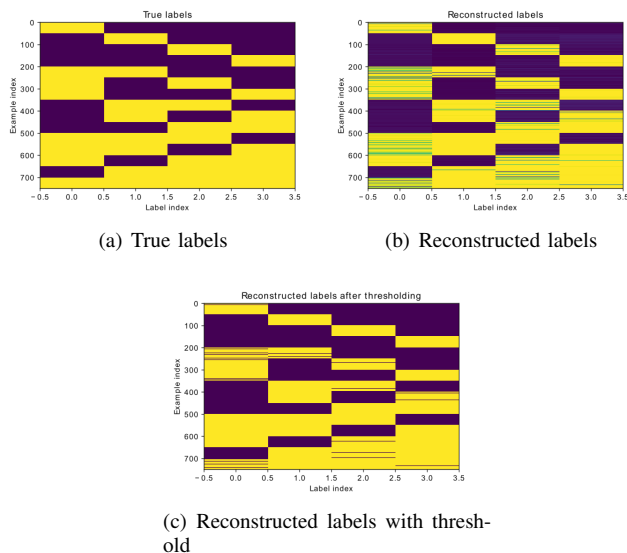


Fig. 4. (a)The left figure is the ground-truth of the labels. (b) The middle figure is the reconstructed labels. (c) The right is the figure showing the reconstructed label with threshold = 0.5.

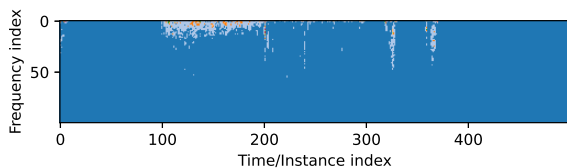


Fig. 5. One training example of ESC-10 data of 5 concatenated instances, respectively with labels as "Sneezing", "Sea waves", "Cracking fire", "Sneezing" and "Null".

kNN performed best with $k = 7$. For MIML-SVM, we tested both linear and RBF kernel variants. The Deep MIML implementation used a reduced VGG architecture [33] (1/5 of the original depth) with batch size 64. WSDL was configured with window size 100, sparsity constraint $N = 100$, $\lambda = 0.1$, and 2 atoms per class. Our WSCDL method used window size 95, $\lambda = 0.1$, $\eta = 0.01$, $\mu = 0.1$, with average pooling and cross-entropy loss. Table II presents the averaged results from 5 independent test runs. The performance differences stem from each method’s alignment with the problem structure. For fair comparison, we used a dynamic threshold (mean of maximum and minimum predicted probabilities) instead of a fixed 0.5 threshold.

WSDL, Deep MIML, and MIML-kNN performed near random guessing due to various limitations: MIML-kNN’s distance-based approach struggles with the high intra-class variance; Deep MIML suffers from insufficient training data

and expects instances as small image patches rather than boundary-spanning segments; WSDL lacks our crucial \mathbf{W} term for projecting instance labels to bag labels, instead using a simple union operation that makes it overly dependent on per-instance labels.

WSDL, Deep MIML, and MIML-kNN performed near random guessing due to several limitations: MIML-kNN struggles with high intra-class variance; Deep MIML suffers from insufficient training data and mismatched model assumptions; WSDL lacks our crucial \mathbf{W} term for projecting instance labels to bag labels. Our method’s incorporation of \mathcal{D}_0 effectively filters background noise, enhancing performance.

MIML-SVM and our WSCDL approach significantly outperformed other methods. MIML-SVM aligned well with the problem structure, though interestingly, its non-linear kernel variant showed no improvement over the linear version. Our algorithm achieved the highest accuracy (0.6330) among all compared methods, despite the inherent challenges of weakly supervised learning on this complex dataset.

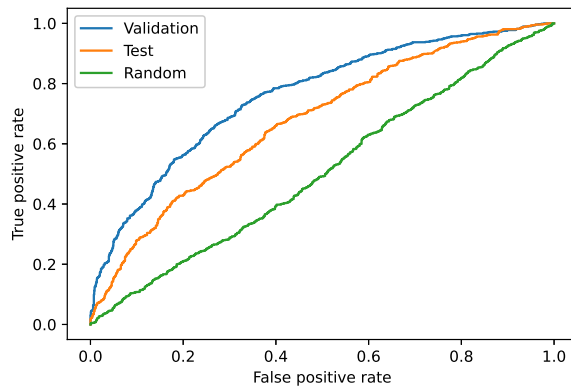


Fig. 6. ROC curves comparing classification performance on ESC-10 dataset. The blue curve shows the middle-ranking result from 5-fold validation (AUC=0.75), while the orange curve represents the middle-ranking test result (AUC=0.67). The green diagonal line indicates random guessing performance (AUC=0.5) for reference.

Fig. 6 presents the Receiver Operating Characteristic (ROC) curves demonstrating our classifier’s performance. For clarity and representative visualization, we selected the median-performing curve from our 5-fold validation (blue curve, AUC=0.75) and the median result from our 5 independent test runs (orange curve, AUC=0.67). The diagonal green line represents random classification performance (AUC=0.5) for reference. The performance gap between validation and test

results is consistent with the inherent challenges of weakly supervised learning on this dataset, where instance-level label ambiguity creates variability in classification outcomes. This performance pattern was observed across all compared algorithms, confirming that our method maintains competitive performance despite the challenging nature of the ESC-10 dataset in a weakly supervised setting.

VIII. CONCLUSION

We proposed a novel CDL framework for weakly supervised MIML classification. Our approach demonstrates superior performance when training data is limited or when individual instances lack clear labels. Key innovations include: (1) a shared background dictionary that enhances discriminative power of class-specific features, (2) an efficient Block Proximal Gradient method with Majorization (BPG-M) that ensures fast convergence despite the computational demands of convolution operations, and (3) a projection mechanism that significantly improves bag-level label prediction accuracy. While our model extends to tensor data, current implementation is limited to 2D optimization due to majorization matrix constraints. Future work will focus on improving instance-level label predictions and extending the optimization method to handle higher-dimensional tensor data directly.

REFERENCES

- [1] M. Aharon, M. Elad, and A. Bruckstein, "K-svd: An algorithm for designing overcomplete dictionaries for sparse representation," *IEEE Trans. Signal Process.*, vol. 54, no. 11, pp. 4311–4322, 2006.
- [2] A. Bruckstein, D. Donoho, and M. Elad, "From sparse solutions of systems of equations to sparse modeling of signals and images," *SIAM Review*, vol. 51, no. 1, pp. 34–81, 2009.
- [3] Y. Xu and W. Yin, "A fast patch-dictionary method for whole image recovery," *Inverse Problems and Imaging*, vol. 10, pp. 563–583, 2016.
- [4] S. Shekhar, V. M. Patel, and R. Chellappa, "Analysis sparse coding models for image-based classification," in *Int. Conf. on Image Process.*, 2014, pp. 5207–5211.
- [5] M. Yang, L. Zhang, X. Feng, and D. Zhang, "Fisher discrimination dictionary learning for sparse representation," in *Proc. Int. Conf. Computer Vis.*, Barcelona, Spain, Nov. 2011, pp. 543–550.
- [6] W. Tang, A. Panahi, H. Krim, and L. Dai, "Analysis dictionary learning: an efficient and discriminative solution," in *Proc. Int. Conf. Acoust. Speech Signal Process.*, May 2019, pp. 3682–3686.
- [7] J. Deng, W. Dong, R. Socher, L.-J. Li, K. Li, and L. Fei-Fei, "ImageNet: A Large-Scale Hierarchical Image Database," in *Conf. on Computer Vis. and Pattern Recognition*, 2009.
- [8] I. Dokmanic, K. Kumanan, Y. M. Lu, and R. Vidal, "Dicodile: Distributed convolutional dictionary learning," in *IEEE Int. Conf. on Acoustics, Speech and Signal Processing (ICASSP)*, 2021, pp. 4230–4234.
- [9] R. Liu, L. Ma, J. Zhang, X. Fan, and Z. Luo, "Multi-modal convolutional dictionary learning," in *Proc. of the IEEE/CVF Conf. on Computer Vision and Pattern Recognition*, 2022, pp. 11 363–11 372.
- [10] T. G. Kolda, D. Hong, and J. A. Duersch, "Tensor convolutional dictionary learning with cp low-rank activations," *SIAM Journal on Mathematics of Data Science*, vol. 4, no. 3, pp. 1100–1125, 2022.
- [11] Y. Zhang, Q. Li, Y. Guo, and D. Zhang, "Deepm2cdl: Deep multi-scale multi-modal convolutional dictionary learning network," *IEEE Trans. Pattern Anal. Mach. Intell.*, vol. 45, no. 2, pp. 2287–2302, 2023.
- [12] B. Chen, J. Li, B. Ma, and G. Wei, "Convolutional sparse coding classification model for image classification," in *2016 IEEE Int. Conference on Image Processing (ICIP)*, Sep. 2016, pp. 1918–1922.
- [13] J. Jin and C. L. P. Chen, "Convolutional sparse coding for face recognition," in *2017 4th Int. Conf. on Info., Cyber. and Comput. Social Systems (ICCSS)*, Jul. 2017, pp. 137–141.
- [14] Z. You, R. Raich, X. Z. Fern, and J. Kim, "Weakly supervised dictionary learning," *IEEE Trans. Signal Process.*, vol. 66, no. 10, pp. 2527–2541, May 2018.
- [15] I. Y. Chun and J. A. Fessler, "Convolutional dictionary learning: Acceleration and convergence," *IEEE Trans. Image Process.*, vol. 27, no. 4, pp. 1697–1712, Apr. 2018.
- [16] H. Chen, S.-J. Kim, and T. Chatt, "Discriminative dictionary learning for mixture component detection with application to rf signal recognition," in *Proc. Asilomar Conf. Signals Syst. Comput.*, 2018, pp. 835–839.
- [17] H. Chen and S.-J. Kim, "Robust rf mixture signal recognition using discriminative dictionary learning," *IEEE Access*, vol. 9, pp. 141 107–141 120, 2021.
- [18] R. Grosse, R. Raina, H. Kwong, and A. Y. Ng, "Shift-invariant sparse coding for audio classification," in *Proc. of the 23rd Conf. Uncertainty Artificial Intell.*, Vancouver, BC, Canada, Jul. 2007, pp. 149–158.
- [19] F. Heide, W. Heidrich, and G. Wetzstein, "Fast and flexible convolutional sparse coding," in *Conf. on Computer Vis. and Pattern Recognition*, 2015, pp. 5135–5143.
- [20] Z.-H. Zhou and M.-L. Zhang, "Multi-instance multi-label learning with application to scene classification," in *Advances in Neural Info. Process. Syst.*, B. Schölkopf, J. Platt, and T. Hoffman, Eds., vol. 19. MIT Press, 2007, pp. 1609–1616.
- [21] M. Zhang, "A k-nearest neighbor based multi-instance multi-label learning algorithm," in *2010 22nd IEEE Int. Conf. on Tools with Artificial Intell.*, vol. 2, 2010, pp. 207–212.
- [22] C.-C. Chang and C.-J. Lin, "Libsvm: A library for support vector machines," *ACM Trans. Intell. Syst. Tech.*, vol. 2, no. 3, May 2011.
- [23] J. Feng and Z.-H. Zhou, "Deep miml network," in *Proc. of the Thirty-First AAAI Conf. on Artificial Intell.*, ser. AAAI'17. AAAI Press, 2017, pp. 1884–1890.
- [24] T. H. Vu and V. Monga, "Fast low-rank shared dictionary learning for image classification," *IEEE Trans. Image Process.*, vol. 26, no. 11, pp. 5160–5175, Nov. 2017.
- [25] S. Boyd, N. Parikh, E. Chu, B. Peleato, and J. Eckstein, "Distributed optimization and statistical learning via the alternating direction method of multipliers," *Foundations and Trends in Machine Learning*, vol. 3, no. 1, pp. 1–122, 2010.
- [26] G. Peng, "Adaptive admm for dictionary learning in convolutional sparse representation," *IEEE Trans. Image Process.*, vol. 28, no. 7, pp. 3408–3422, 2019.
- [27] A. Khamparia, D. Gupta, N. G. Nguyen, A. Khanna, B. Pandey, and P. Tiwari, "Sound classification using convolutional neural network and tensor deep stacking network," *IEEE Access*, vol. 7, pp. 7717–7727, 2019.
- [28] I. Y. Chun and J. A. Fessler, "Convolutional analysis operator learning: Acceleration and convergence," *IEEE Trans. Image Process.*, vol. 28, no. 11, pp. 5323–5337, 2019.
- [29] A. Beck and M. Teboulle, "A fast iterative shrinkage-thresholding algorithm for linear inverse problems," *SIAM J. Imag. Sci.*, vol. 2, no. 1, pp. 183–202, 2009.
- [30] S. Boyd and L. Vandenberghe, *Convex Optimization*. USA: Cambridge University Press, 2004.
- [31] J.-F. Cai, E. J. Candès, and Z. Shen, "A singular value thresholding algorithm for matrix completion," *SIAM J. Optim.*, vol. 20, no. 4, pp. 1956–1982, 2010.
- [32] K. J. Piczak, "Esc: Dataset for environmental sound classification," in *Proc. of the 23rd ACM Int. Conf. on Multimedia*, Oct. 2015, pp. 1015–1018.
- [33] K. Simonyan and A. Zisserman, "Very deep convolutional networks for large-scale image recognition," in *3rd Int. Conf. on Learning Representations, ICLR 2015, San Diego, CA, USA, May 7-9, 2015, Conf. Track Proc.*, 2015.